Research Journal of Chemical Sciences ISSN 2231-606X
Vol. **8(4),** 1-14, April **(2018)** *Res. J. Chem. Sci.*

Characterization and evaluation of the adsorption capacity of dichromate ions by a clay soil of Impfondo

Moutou J.M.[1,2*], Bibila Mafoumba C.[2], Matini L.[1,2], Ngoro Elenga F.[2] and Kouhounina L.[2]
[1]Ecole Normale Supérieure Université Marien Ngouabi B.P. 69 Brazzaville, Congo
[2]Laboratoire de Chimie Minérale et Appliquée, Faculté des Sciences et Techniques, Université Marien Ngouabi B.P. 69 Brazzaville, Congo
jmsbmout@yahoo.fr

Available online at: www.isca.in, www.isca.me
Received 2nd November 2017, revised 10th March 2018, accepted 15th April 2018

Abstract

This work had as a general objective the evaluation of adsorption capacity of dichromate ions by clay collected in the Impfondo locality. The mineralogy of this soil was determined by X-Ray diffraction, Infrared spectroscopy and differential thermal analysis and thermogravimetry analysis. The geotechnical (Atterberg limits and grain-size distribution) and the chemical properties (chemical composition, CEC, Tamm Fe and Mehra-Jackson Fe) were also studied. The surface properties (specific surface area and zero charge point) were evaluated. The adsorption isotherms and adsorption kinetics were carried out. Impf clay consists mainly of kaolinite, but also illite, quartz, goethite, anatase, rutile and hematite. The particle size distribution corresponds to clay texture and offers the adsorption possibility. The surface properties (CEC, adsorption isotherm, adsorption kinetics, point of zero charge) have permitted to evaluate the adsorption capacity of Impf clay. This study showed that the adsorption isotherm of dichromate can be interpreted by the Langmuir and Freundlich models. Both models are to the extent of acceptability. The Freundlich model was used to calculate the Freundlich constant and the heterogeneity factor. This study made it possible to conclude that the adsorption yield of dichromate on Impfondo kaolinite is low; it increases with the mass of the introduced kaolinite. And at a mass of 0.5 g of kaolinite in 25 ml of dichromate solution, the adsorption sites become saturated and the equilibrium is reached. Following adsorption kinetics, the adsorption of dichromate is described by the second-order model. It was possible to determine the rate constant and the adsorption capacity of equilibrium dichromate ions. The adsorption of dichromate is favored when the pH of the environment is much lower than that of the zero charge point of the kaolinite.

Keywords: Clay, mineralogical characterization, size-particle distribution, adsorption, dichromate ions, specific surface area.

Introduction

Industrial activities are generally a very important source of pollution and contribute to the degradation of the environment. The release of heavy metals in nature causes many chemical reactions between the cations of these metals and some ligands in the environment. This is the case of chromium ions in the aquatic environment which react with oxygen to form chromate and dichromate, thereby modifying the chemical composition and physicochemical properties of water. Several researchers have been interested in the adsorption of heavy metal cations by solid adsorbents[1-5], and few have been interested in the adsorption of the complexes formed by these metals[6,7]. Several studies have shown the anti-polluting role of clays[8]. Nowadays the applications of clays are constantly growing, and they are used as adsorbents in the elimination of micro pollutants in environment. This is justified by the presence of negative charges on the surface, the possibility of cation exchange, the large specific surface area and their availability in nature[5].

The quantities of chromium detected in groundwater and surface waters in Brazzaville could be at risk. Indeed, in a study of groundwater in Mayanga quarter of Brazzaville, Sita-Keba observed concentrations of Cr(VI) relatively higher than the WHO standards[9]. Nimy observed levels of Cr(VI) superior to the WHO standards in the waters of the national company of distribution of water in Brazzaville[10]. In other area of Brazzaville, in particular Poudriere quarter, groundwater showed higher concentrations of Cr(VI) with the WHO standards. chromium in its hexavalent form, deemed the most toxic form, is involved in the pollution of surface water, by its use in many industries (electroplating, chemical industry, industry of pigments) and as anti-corrosion agents[11-13]. Cr(VI) shows a higher than Cr(III) harmful; potassium chromed experimentally disrupts the growth of algae and as soon as the concentration of $0.5 mgl^{-1}$ in the middle, reduced photosynthesis, reduces the biomass in Chlorella pyrenoidosa as showed by the works of Meisch and Schmitt-Beckmann[14]. Many epidemiological studies have shown that occupational exposure of humans to the chromates cause growth in respiratory cancers[15-17]. Ultraviolet light associated with hexavalent chromium in drinking water stimulate significantly the formation of skin cancers compared to UV alone in mice[18]. Chromium in its hexavalent form is toxic for reproduction[19,20]. Allergic contact dermatitis occurs often as result of dermal exposure to hexavalent chromium[21]. A study revealed that a

0.25% of dichromate solution can cause positive allergic reactions[22].

Consider the elimination of chromium in the groundwater by adsorption requires effective adsorbents. Therefore the study of local clays could open up opportunities to find the adsorbents to remove chromium in waters.

Thus, the general objective of this work is the characterization and the evaluation of chromium adsorption capacity of a clay soil collected at Impfondo locality.

X-ray diffraction will be used for identification of minerals present in this soil. Consolidate the identification, we will use Fourier Transform infra-red spectroscopy in mode diffuse reflectance, differential thermal analysis and thermogravimetry analysis The geotechnical (Atterberg limits and grain-size distribution) and the chemical properties (chemical composition, CEC, Tamm Fe and Mehra-Jackson Fe) will be also studied. The surface properties (specific surface area and zero charge point) will be evaluated. The adsorption isotherms and adsorption kinetics will be carried out.

Material and methods

Location of sampling site: Impfondo is a village in the northeast of the Republic of Congo, capital of the Likouala Department. It is located on the Ubangi River (Figure-1). The coordinates are 1°37'12 "North, 18°03'18" East and the altitude is 326m.

Figure-1: Localisation of Impfondo locality[23].

Pedological point of view, the region is characterized by ferralithiques and alluvial hydromorphic soils[23]. The sampling site is 4km from the port and on the edge of the Ubangi River. Samples are taken during the dry season. Indeed during the rainy season floods cover the natural soil profile.

Physicochemical and mineralogical characterization: The limits of Atterberg were measured according to the standards[24]. The proportions of the following particle classes are determined according to the standard NF P94 056 and NF P94 057[25].

The X-ray pattern was recorded on a raw sample using a 'PANALYTICAL X'PERT PRO' 'K α_1 (θ-2θ) diffractometer using Cu Kα_1 radiation (45kV, 40mA) in the Institute of Condensed Matter Chemistry of Bordeaux (ICMCB).

The chemical analysis of the major elements was carried out according to the procedure of Carignan et al.[26] at CRPG Nancy.

The extraction of iron and aluminium is done according to two methods: i. Mehra Jackson method[27], ii. Tamm method[28].

The iron and aluminium contents, extracted from these two techniques were carried out by atomic emission spectrometry in induced plasma of argon (ICP-AES).

Diffuse Reflectance Infra-red Fourier Transform Spectroscopy (DRIFTS) was performed over a wave number domain between 600 and 4000/cm using a Bruker IFS 55 spectrometer equipped with a broad band detector of MCT type (Mercury and Cadmium Tellurium) cooled at 77K and with an accessory of diffuse reflection (Harrick Corporation).

The powdered sample was diluted in KBr (50 mg of sample in 350mg of KBr). The spectra were recorded by accumulating 200 scans at a 2.0/cm resolution.

The Differential Thermal Analysis (DTA) and Thermo Gravimetry (TGA) were carried out with a SETARAM device coupled with a thermobalance. The heating rate was 10°C./min.

The specific surface area of the crude fraction and the fine fraction of this sample was determined from the adsorption isotherms of methylene blue[29]. The maximum quantity M_f of the methylene blue adsorbed is determined in millimoles per 100g of material, from the level of the adsorption isotherm. Knowing the surface A_m (135Å^2) of a molecule of methylene blue and the maximum quantity M_f, the specific surface area was estimated by the following equation:

$$S = M_f A_m 6.02.10^{-2} m^2 g^{-1} \quad (1)$$

The Cation Exchange Capacity was determined on the raw sample and on the fine fraction according to METSON[30]. It consists of three stages: i. the sample is first saturated with ammonium ions (NH_4^+) by successive percolations of a 1mol/L solution of ammonium acetate ($CH_3CO_2NH_4$). His buffering capacity makes it possible to reduce the pH of the environment to about 7, which is one of the essential characteristics of this method. ii. the excess of ammonium ions are removed by percolation of ethyl alcohol, after which they are exchanged with a 1 mol/L sodium chloride solution.

The displaced ammonium ions are assayed by spectrocolorimetry on the previous solution, after filtration. The concentrations found are converted to cmol+/kg (centimol of positive charge per kilogram of soil). Taking test is 2.5g of soil sifted to 2mm.

Adsorption of dichromate ion on the IMPF sample: Kinetics of adsorption: The kinetics of adsorption of dichromate ions by this kaolinite was observed by mixing in several erlenmeyers of 250ml, 0,5g of the kaolinite and 25ml of 122,3mg/l dichromate solution. The pH of the mixture was adjusted to 1,99. The solutions were stirred for 2h, and every 20min, the samples were taken. This allowed the evolution of the dichromate content to be monitored.

Adsorption isotherm: The method chosen consists of maintaining constant the concentration of the adsorbate and then varying the mass of the adsorbent[31]. In 7 erlenmeyer flasks of 250 ml each, 0.1g; 0.2g; 0.3g; 0.4g; 0.5g; 0.6g and 0.7g of the kaolinite sample was introduced successively, and 25ml of the 4.10^{-4}M of dichromate solution. The pH of the mixtures was adjusted to 1.99. The mixtures were stirred at 25°C for 3hours, then settled overnight and then centrifuged for 30min. The supernatant solutions were analyzed for equilibrium dichromate concentrations by spectrophotometry. The adsorption capacities of IMPF sample was calculated using equilibrium studies. The mass balance equation for this process at equilibrium is given by equation (2).

$$Q_e = (C_0 - C_e)\,{}^{V}/_{m} \qquad (2)$$

Where: Q_e(mg/g) is the adsorbent capacity, C_0(mg/L) is the initial concentration, C_e(mg/L) is the final or equilibrium concentration, V is the experimental solution volume (L), and m is the adsorbent mass (g).

Point of zero charge (PZC): The principle used in this work consists in titrating the clay suspensions with KCl with hydrochloric acid (HCl) or sodium hydroxide solution (NaOH), in order to monitor the pH of the suspension of clay at different ionic forces as a function of the quantity of hydrochloric acid and added base[32]. Indeed, six suspensions of clay were prepared by mixing 1.5g of the IMPF sample with 25mL of a potassium chloride (KCl) solution at various concentrations: two suspensions with a solution of 0.1NKCl, two others with 0.01N KCl and two solutions with a solution of 0.001NKCl. After stirring for 24hours, the suspensions are subjected to pH-metric titration by the 0.1NHCl solution or the 0.1NNaOH solution using the pH meter. The point of zero charge (PZC) is determined from the intersection of the titration curves of the different suspensions.

Effect of pH: The influence of pH on the adsorption of dichromate ions was studied by introducing in the erlenmeyer flasks different masses of kaolinite and 25ml of the dichromate solution at pH 5.03 and 1.99. The mixtures are first stirred using the magnetic stirrers for 120minutes. After decantation, the supernatants are centrifuged for 30min.

Results and discussion

Limits of Atterberg: The limits of Atterberg are shown in the Table-1.

Table-1: limits of Atterberg of IMPF sample.

Sample	IMPF
Liquidity limit W_L	50,08
Plasticity limit W_P	22,08
Plasticity index I_P	28

This result, which shows the plasticity index IP=28, qualifies this sample as a inorganic clay of medium plasticity using the CASAGRANDE chart[33] (Figure-2).

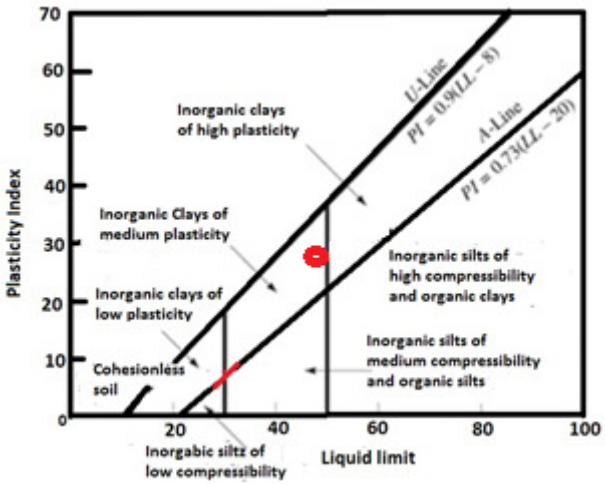

Figure-2: Positioning of IMPF sample in CASAGRANDE chart.

Particle size analysis: The results of particle size analysis of IMPF sample are shown in the Table-2.

Table-2: Particle size analysis of IMPF sample

Sample	Argile %	Limon %	Sable %	Total %
IMPF	80	8	12	100

This result reveals that the IMPF sample has the clay texture. With 80% of clay, IMPF sample would present a high capacity to adsorb the micropollutants. Indeed, the adsorption intensity depends to size of particles[34].

XRD pattern of IMPF sample: The Figure-3 shows the XRD pattern of IMPF sample. Examination of the XRD pattern of the

IMPF sample revealed the presence of the following minerals: kaolinite, illite, quartz, goethite, anatase, rutile and hematite[35,36]. With regard to the heights of the peaks, kaolinite is the most abundant clay mineral.

The height of the peaks related to goethite and the hematite indicated the considerable presence of the iron in that sample. Titanium oxides (rutile and anatase) are also relatively non-negligible.

In the XRD pattern of an ordered kaolinite, the interval ranging from 19° to 23° presents usually three distinct peaks while the increase in disorder makes that the sequence of 02*l*, 11*l* reflections in the range 20°-33° becomes increasingly blurred until with halloysite only a smooth diffraction band with the superimposed 002 basal reflection is obtained[37]. As we observe one peak in this interval, we can think that the kaolinite is disordered. Figure-4 represents the XRD pattern of the sample heated to 500°C.

We can observe the disappearance of the peak at 7,23Å. The kaolinite is transformed into metakaolinite. The persistence of the peak at 10,0Å confirms the presence of illite.

Chemical properties of the IMPF sample: The Table-3 gives us the chemical properties.

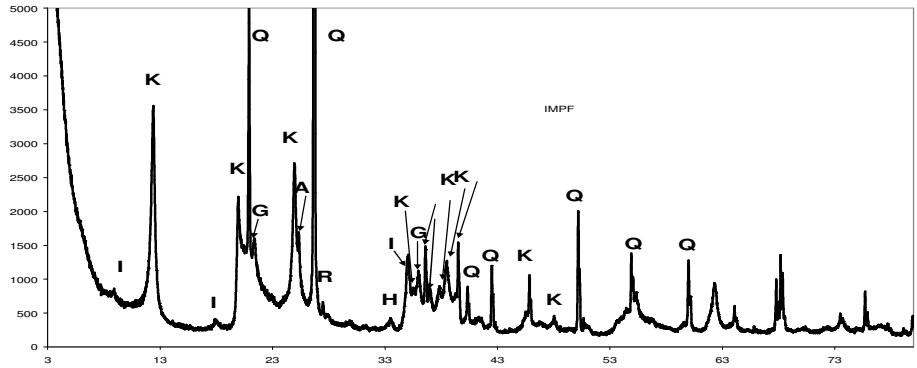

Figure-3: XRD pattern of IMPF sample.
(I=illite, K=kaolinite, G=goethite, Q= quartz, A=anatase, R=rutile, H=hematite)

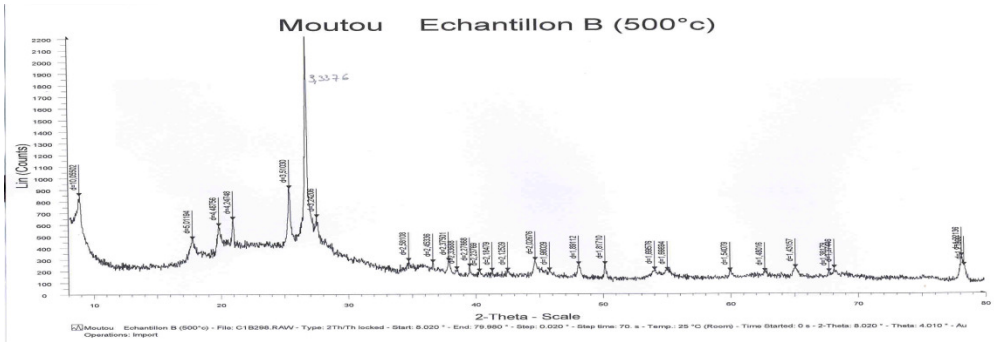

Figure-4: XRD pattern (sample heated to 500°C).

Table-3: Chemical properties.

SiO_2	Al_2O_3	Fe_2O_3	MnO	MgO	CaO	Na_2O	K_2O	TiO_2	P_2O_5	P.F.
52,34	25,07	6	0,02	0,25	0,04	0,05	0,66	2,03	0,07	12,47

Organic matter	Organic carbon	Total nitrogen	Organic matter
	0,229%	0,0275%	0,397%

CEC	8,8 cmol+/kg	9,

Tamm Fe	Tamm Al	Mehra-Jackson Fe	Mehra-Jackson Al
0.077%	0,144%	2,96%	0,377%

The SiO_2 / Al_2O_3 ratio in the IMPF sample is 2,1. It is higher than the ratio in kaolinite (1,2) that is the most predominant clay mineral soils. This corresponds to a significant presence of quartz in The IMPF.

The rate of alkaline and alkaline earth oxides is negligible. Indeed, this soil flooded during the rainy season which last six months, is highly leached. The K_2O rate relatively important would correspond to presence of illite. These values are lower than in an illitico-kaolinic clay[38] and comparable to the kaolinic clay LOU[39]. The non-negligible MgO content in the IMPF sample would possibly correspond to the very low presence of smectites or T-O-T mineral in which magnesium substitutions of aluminum would occur in the octahedral layers.

The Tamm method provides information on the iron present in the amorphous state in the sample, often in the form of complexes of organic compounds[40].

In the IMPF sample, the amount of the amorphous iron is very low (0,077g /100g). The Mehra Jackson method applied to the same sample shows 2,96g 100g of crystallized and amorphous iron. The combined results of Iron Tamm and Iron Mehra Jackson methods led to a percentage of 3,04% free iron. Moreover, the chemical analysis shows 6% of iron oxide (Fe_2O_3), which corresponds to 4,2% of total iron. The calculation of the percentage of structural iron, gives 1,16%. The free iron represents 72,4% of total iron. The importance of free iron would justify the manifestation of the peaks relating to the goethite and hematite on the IMPF XRD pattern.

Loss on ignition is important for IMPF (12,47). It depends on the content of the clay species and the significant presence of goethite.

Differential and gravimetric thermal analysis: The Figure-5 gives us the DTA curve of IMPF sample:

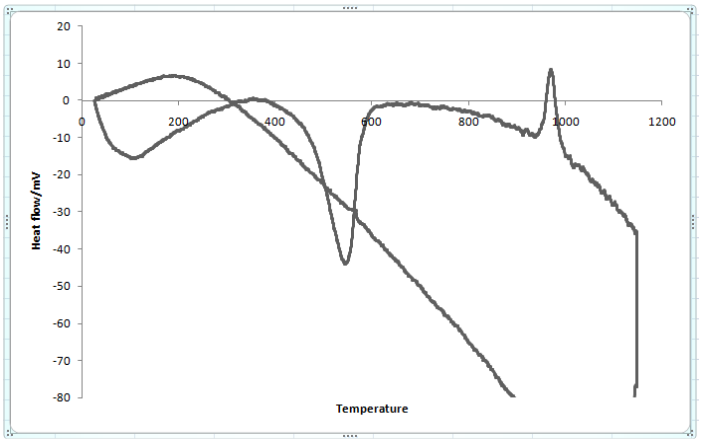

Figure-5: DTA curve.

Examination of this figure reveals the presence of an endothermic peak at approximately 100°C, an endothermic peak at 535°C and an exothermic peak at 971°C. In relation with the results of the XRD, the first peak corresponds to the departure of the hygroscopic water (adsorbed), the second can be attributed to the dehydroxylation of the kaolinite which turns into metakaolinite and the exothermic peak to the structural reorganization of metakaolinite to mullite[41,42]. Unlike the DTA curves of LOU and MOU clays[38,39] which have relatively large rates of sand, peak linked to the reversible quartz transformation is not visible on the DTA curve of IMPF.

The following Figures-6 and 7 represent the TGA and DTG curves.

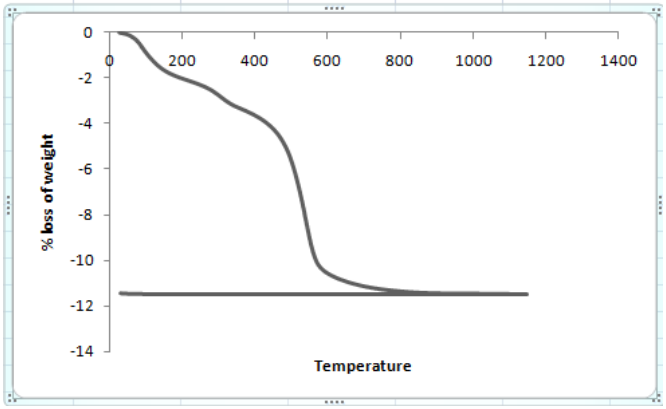

Figure-6: TGA curve.

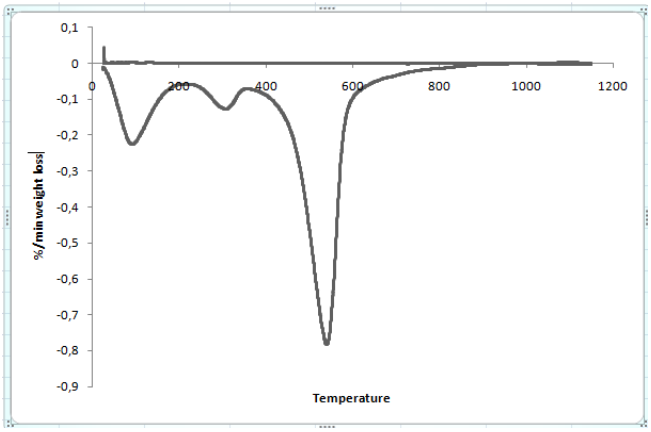

Figure-7: DTG curve.

The analysis of these curves reveals three phenomena causing weight loss: i. Around 91°C of the order of 2.2%, ii. Around 295°C of the order of 1.1%, iii. Around 535°C of the order of 7.7%.

The losses of weight around 91°C and 535°C are related to the departure of adsorbed and the deshydroxylation of kaolinite. The loss of weight around 295°C could be related to the presence of goethite. Indeed, it is indicated that goethite undergoes a hematite transformation at these temperatures[43]. The weight loss of 7.7% corresponding to the dehydroxylation of the kaolinite leads us to estimate a kaolinite content (55%) in this IMPF sample.

Mineralogical balance: Mineralogical balance is carried out according the formulae[44,45]

$$T(a) = \sum M_i P_i(a) \quad (3)$$

Where: T(a)=Mass percent of the element oxyde a in the sample, Mi=Mass percent of the mineral "i" in the studied material, Pi(a) =Massic amount of the oxyde of the "a" element in the mineral "i" deduced from the ideal formula of the minéral i.

Table-4: Mineralogical balance of IMPF sample.

Kaolinite	Illite	Quartz	Hématite	Rutile
61,79%	5,59%	27,27%	4,34%	2,03%

Referring to the chemical analysis, the IMPF clay soil contains a significant clayey species rate (kaolinite and illite = 67,38%). Therefore the IMPF sample presents a significant potential as adsorbent. On the other hand, considering weight loss revealed by thermogravimetry and associated to the deshydroxylation of kaolinite, this latter would be less important (55%). But if the rate of kaolinite decreased, illite rate would be increased since the total content of clay species remains constant (67,38%), therefore the illite rate will be 12.38%. The kaolinite/illite ratio (4,44) is near to the report of the intensities of the principal peaks in the XRD pattern of the IMPF sample (3603,6/904, 57 = 3,98). 55% would be near the true rate of kaolinite. These values are between the minimum value of the CEC of the kaolinite (5meq/100g) and that of the CEC of the illite (10meq/100g)[46]. These values show a predominance of kaolinite. The CEC of the fine fraction is greater than that of the crude clay. This can be explained by the enrichment of the fine fraction of clay minerals relative to the crude clay soil.

Infra-Red Spectrum: The IR spectrum of IMPF sample is showed in Figure-8.

The range from 3700cm^{-1} to 3600cm^{-1} corresponds to the elongation modes of the OH groups[47]. The IMPF sample shows three intense bands 3696cm^{-1}, 3653cm^{-1} and 3620cm^{-1} in this range.

The kaolinite is the most abundant clay mineral in the IMPF sample. It is indicated that four OH stretching bands are typical of kaolinite[48-50]. The three bands observed on IMPF TFIR spectrum are ascribed to elongation vibrations[51]. Many studies on cristallinity of kaolinite showed that the decrease of order in kaolinite leads to decrease of the bands (three instead four: 3695, 3658 and 3620cm^{-1})[52-54]. The three bands observed in the range 3700-3600cm^{-1} can be assigned to hydroxyl stretching modes. But the kaolinite in IMPF should be disordered. The intense bands at 3420 and 1631/cm are due to the free water molecules[55]. In TFTIS spectrum at 80°C of LOU sample, the intensities of these bands highly decrease[39]. The well defined band at 3435/cm in DRIFTS could reveal small amounts of gibbsite[56]. The very weak percentage of Al Mehra-Jackson does not favor this attribution. The bands at 935cm^{-1} and 915cm^{-1} correspond to the Al-OH-Al and AlO-H deformation vibrations. The bands at 1159 and 1113 cm^{-1} correspond to the symmetrical and asymmetric Si-O mode. The elongation mode of the Si-O bond in kaolinite gives 1021cm^{-1}.

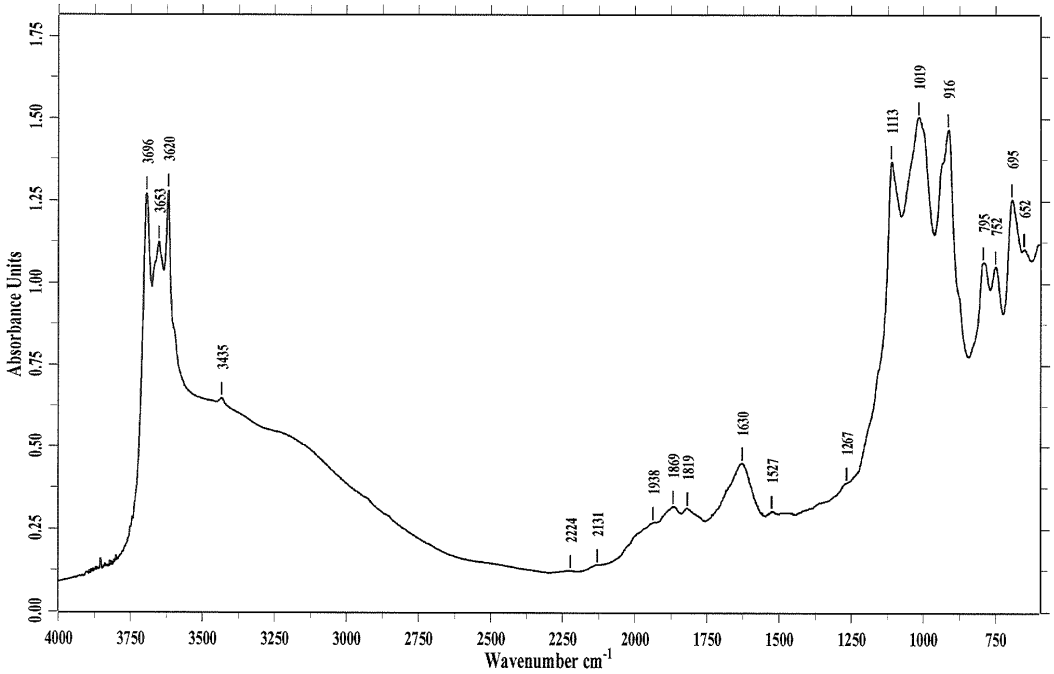

Figure-8: infra-red spectrum of IMPF sample.

The band 752 and the band 795 due to the silica in the samples are quite distinct in IMPF.

A study by infrared spectroscopy of kaolinite-quartz mixtures reveals that the quartz has two bands around the frequency 1010 cm^{-1} [57]. The band to 652 cm^{-1} expresses the presence of the goethite[58].

The band at 2131 cm^{-1} is attributed to the deformation-rotation combination of the water molecule[59].

Specific surface: The Figure-9 gives us the adsorption isotherms of BM on fine fraction and crude clay of IMPF sample.

The Table-7 shows the value of the specific surface area of the crude clay soil and that of the clay fraction.

Table-7: specific surface area.

IMPF sample	Crude clay soil	Clay fraction
specific surface area (m^2/g)	69,89	78,83

These values are very higher than the values of clay LOU and MOU which are kaolinitic clays, measured by BET methods (37,0 and 33,7 m^2/g). These clays have the size distribution near the IMPF sample.

Brindley et al. indicate that maximum adsorption of methylene blue, corresponding to complete exchange of the inorganic by the organic ions, occurs with larger amounts of methylene blue than are required for optimum flocculation[29]. In their study the value of M_f is taken as the amounts of methylene blue adsorbed for optimum flocculation. It is considered that the amount of methylene blue adsorbed under these conditions corresponds to coverage of the clay surface with methylene blue molecules[29]. The optimum flocculation is often situated before the curvature on the isotherm. Taking M_f lower to the maximum adsorption we have the following specific surface area 46,8m^2/g (crude clay) and 62,4 m^2/g (fine fraction). The LOU illite and kaolinite content are practically identical to that of IMPF and his BET specific surface is 37m^2/g[39]. The value of IMPF neared the value of kaolinite from Florida[29]. The relatively significant proportion of illite would cause a higher specific surface area of IMPF sample compared to that of kaolinite.

Point of zero charge of IMPF clay sample: The evolution of pH based on the concentration of hydrochloric acid or soda is given in Figure-10 (crude sample) and Figure-11 (fine fraction).

From these curves, the pH of the points of zero charge (PZC) has been determined (4.5 for raw sample and 5.0 for the fine fraction).

Many studies on kaolinite reveal that this latter has PZC around of 3 and even lower to 3. However, the PZC of the oxisols are quite high (4 to 5). Hendershot and Lavkulich showed that iron oxides coating clayey minerals increase the PZC of these[60]. The PZC value of IMPF sample is relatively high because of the large presence of oxides of iron in the soil.

These values are close to that of the zero charge point of kaolinite comparable to that found by Rahajaritompo R. L. (pH_{PCN} = 4.6)[61]. This may be due to the fact that kaolinite is the major mineral species in these clays.

Thus, it may be thought that when the clays are suspended, for pH values below 4.6 the surface of the clay particles is positively charged and can therefore fix the anions.

Adsorption Isotherm: The adsorption isotherm of our study is obtained by plotting the adsorbed amount of dichromate ions Qe (in mg/g) as a function of equilibrium concentration Ce (mg /l) of the dichromate ions (Figure-12).

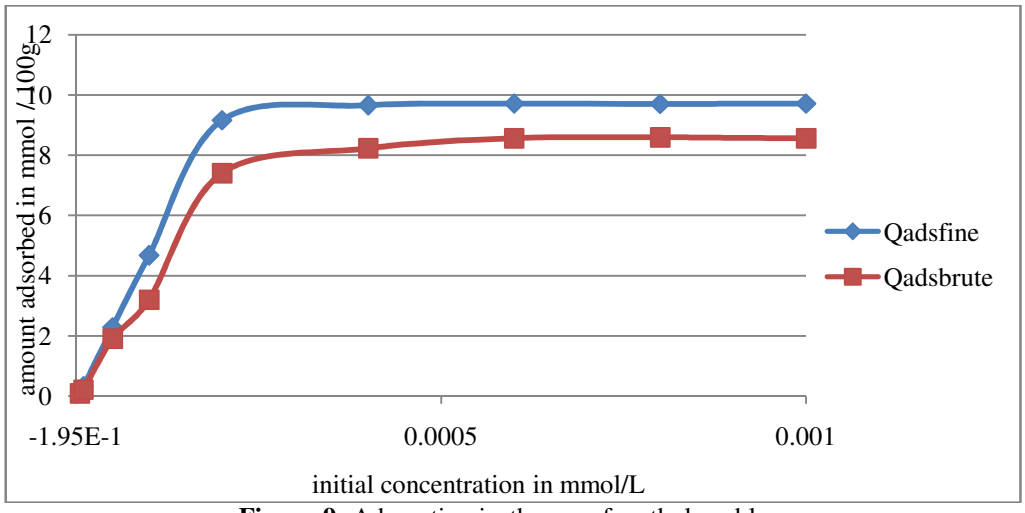

Figure-9: Adsorption isotherms of methylene blue.

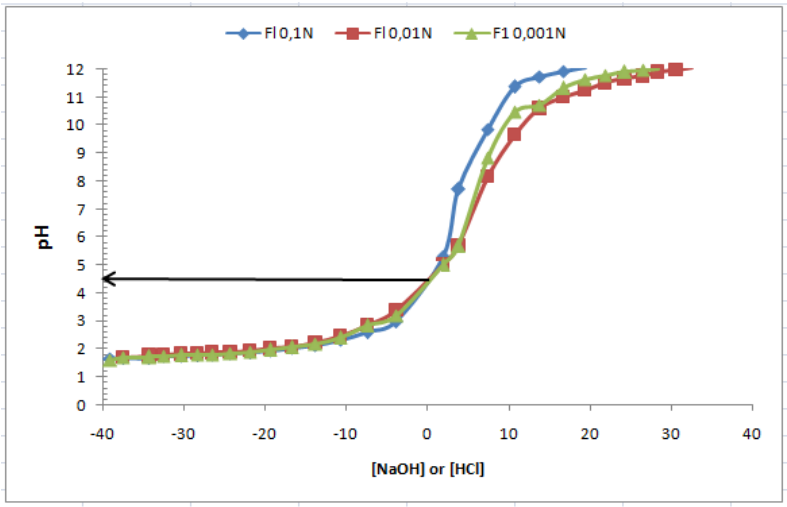

Figure-10: Titration curves of the suspension with the raw clay to various ionic strengths.

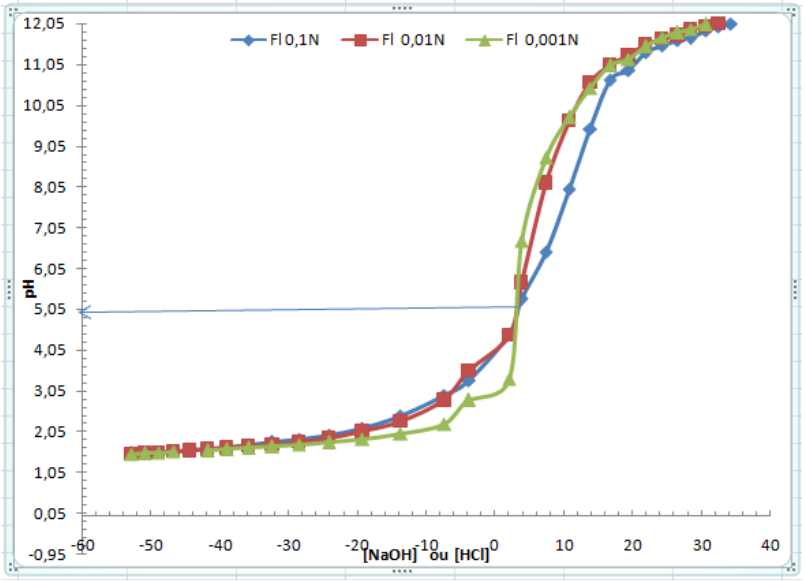

Figure-11: Titration curves of the suspension with the fine fraction to various ionic strengths.

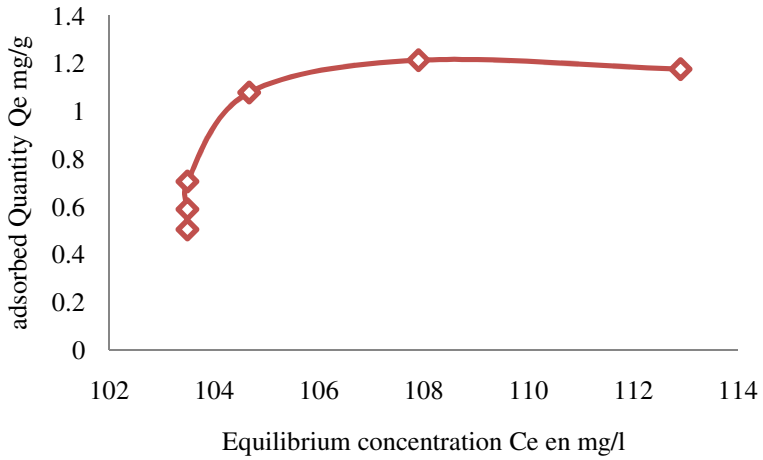

Figure 12: adsorption isotherm of dichromate ions on IMPF sample.

This isotherm corresponds to that of type H[62]. It does not start with zero, and the initial part of this isotherm is vertical. This figure shows that, at low starting concentrations, the adsorption would almost be total. This phenomenon occurs when the interaction between the adsorbed molecules and the surface of the solid is very strong.

Application of the Langmuir model: The linearization according to the simplified model of Langmuir is represented in Figure-13.

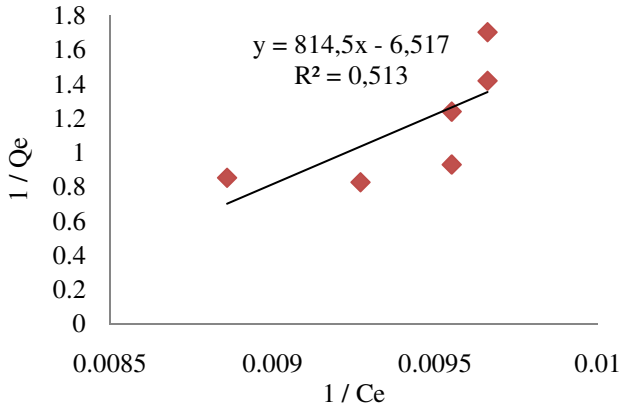

Figure-13: Langmuir model.

The linearized Langmuir equation is $Y = 814.52X - 6.517$.

The plot of that Langmuir equation gives the straight line of the form

$$^1/_{Q_e} = {}^1/_{bC_eQ_m} + {}^1/_{Q_m} \quad (4)$$

Where: $Q_e = (C_o - C_e)V/m$ is the adsorbed quantity of solution (mg/g); C_e is the equilibrium concentration of solution (mg/l); V: volume of solution (liter); *m*: the mass of clay (gram); $Q_m = \left(X^V/_m\right)_o (mg/g)$ is the maximum adsorbed quantity; *b* is the ratio of constants of adsorption rate and desorption rate.

The correlation factor is $\mathbf{R^2}$= 0.5134

Application of the Freundlich model: Determination of the Freundlich constant and the heterogeneity factor.

The Figure-14 shows Ln (Qe) as a function of Ln (Ce) according to the Freundlich model.

The linearized equation of Freundlich is Y = 6.0934X - 28.536.

It gives the straight line of the form

$$Ln(Q_e) = LnK_F + \left({}^1/_n\right)LnC_e \quad (5)$$

Where: $^1/_n$ is the slope; LnK_F is the ordinate at origin.

Therefore, $K_F = -28{,}536$, $K_F = 4{,}04.10^{-13}$, where K_F is constant of Freundlich type, $^1/_n = 6{,}0934$, n= 0.16, so **n < 1**, where **n** is the factor of heterogeneity.

The correlation factor is $\mathbf{R^2}$ = 0.5136

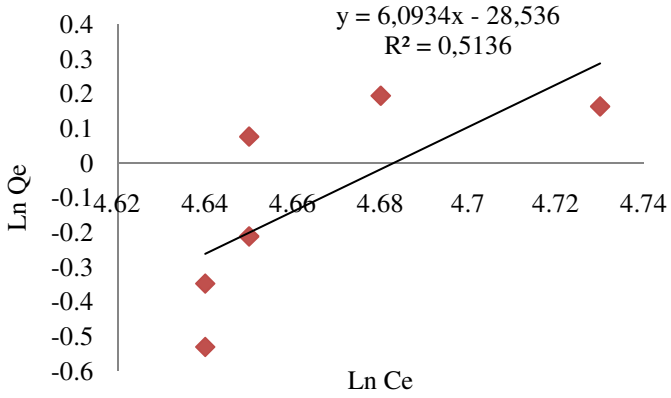

Figure 14: Freundlich model.

This study shows that the Freundlich model gives results similar to the Langmuir model by the correlation factor. Since the value of 1/n is greater than one (1), this confirms the strong interaction between the adsorbent and the adsorbate[63]. So adsorption of dichromate ions by Impfondo clay soil is possible.

The correlation coefficient shows that the Langmuir model and the Freundlich are within the acceptability limit.

Dichromate ions adsorption on the IMPF sample can be described by the Freundlich and also Langmuir equations. But the correlation factors, medium and at the acceptability indicate thus that others phenomena must be taken into account. From the Langmuir point of view, the presence of two clay species (kaolinite and illite) should be at the origin of many adsorption sites[8]. In the case of kaolinite, to first approximation, at least two types of adsorption sites on the edges with the hydroxides =SiOH (tetrahedral sheet) and =AlOH (octahedral sheet) of which the PZC have different values[64]. The more complex structure of the illite is quite similar to that of the Montmorillonite; so presumably it is found several types of sites at the ends of layers, Si - O, Al-OH and Al - O to the Si–O, Al–OH et Al–O at the level of the siliceous and alumina sheets[64]. Therefore, it was possible to apply the Langmuir's modified model for the competitive adsorption. It is a well known fact that the adsorption is subject to a competition between several species[8]. The acidification of IMPF clay suspension can produce the hydroxyl ions by dissolution of iron oxides. The OH- ions could be entering in competition with the dichromate. The application of Freundlich modified model for competitive adsorption would have improved the correlation factor[8].

Kinetics of elimination: Removal of the dichromate ions was monitored as a function of the agitation time of the solutions (Figure-15).

Figure-15 shows that there is equilibrium between 20 and 80 minutes. This equilibrium time corresponds to the maximum efficiency of the dichromate adsorption on the kaolinite. We observe a decrease and then the growth of the dichromate content, which could be explained by the dichromate desorption by the kaolinite. That was observed in the study of the removal of cadmium by adsorption on sodium and calcium bentonites[1], and in the study of the co-adsorption of heavy metals on modified bentonite in the presence of mineral and biological flocculants[2].

Application of the second order kinetic model: The linear plots of second-order kinetic model (equation 3) for dichromate ions are shown in Figures-7.

$$^1/_{Q_t} = {}^1/_{K_2 Q_e^2} + {}^t/_{Q_e} \quad (6)$$

The K_2 and Q_e values are experimentally determined by plotting t/Q_t against t. And a kinetic model is concerned only with the effect of observable parameters on the overall rate.

The correlation coefficient R^2 value for IMPF sorption for dichromate is 0.9788.

The equation of this line is: $Y = 0{,}866X + 0{,}941$

By identification with the equation (3), the equilibrium adsorption capacity is obtained: Qe = 1.1539 mg / g and the rate constant $K_2 = 0.798$ g.mg^{-1}.min^{-1}.

The equilibrium adsorption capacity determined by the second order model (1.1539 mg / g) is very close to that determined experimentally (1.1317 mg / g).

Elimination efficiency: These results are obtained by following the evolution of the adsorbed amounts of the dichromate ions as a function of the mass of the kaolinite. The removal efficiency is calculated from the following equation:

$$(\%)removal = (C_o - C_e)x\ 100/C_o \quad (7)$$

where C_0 and C_e are the initial and equilibrium concentrations (mg/L) respectively

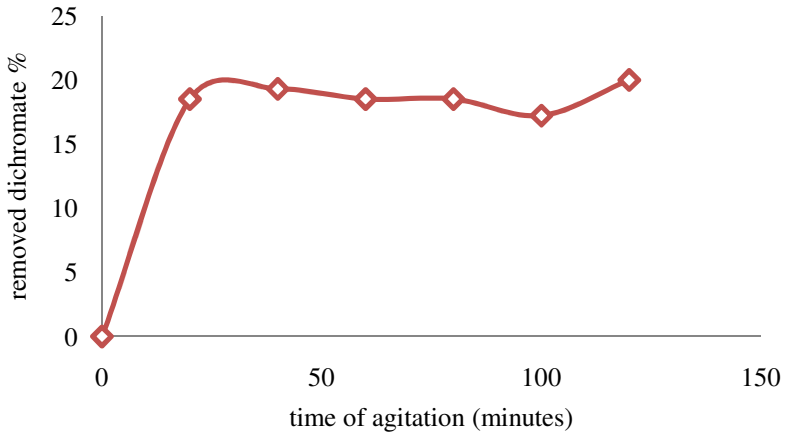

Figure-15: Monitoring of elimination efficiency as a function of agitation time.

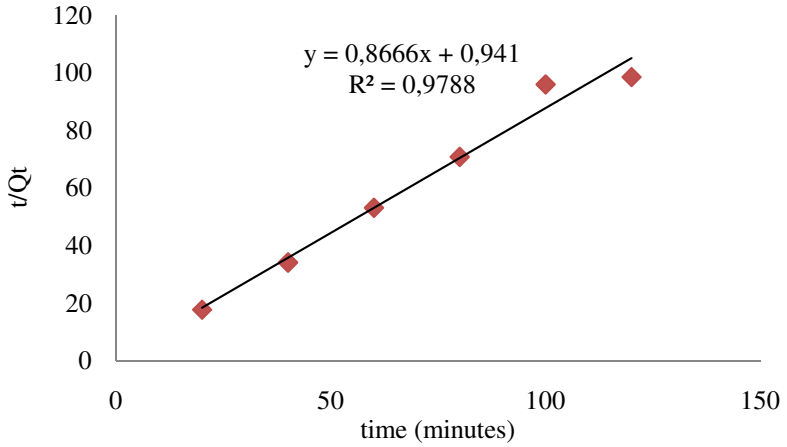

Figure-16: Determination of the adsorption capacity at equilibrium and of the rate constant of adsorption.

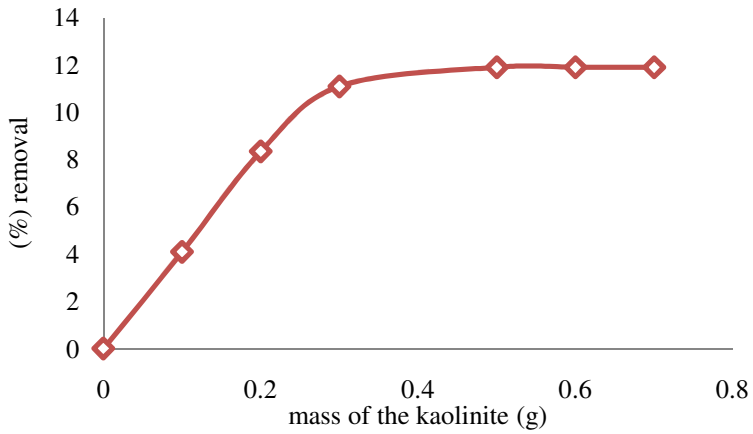

Figure-17: Influence of the mass of the kaolinite on the removal efficiency of the dichromate ions.

The retention of the dichromate ions increases with the mass of the kaolinite and we also observe the appearance of a plateau corresponding to a maximum efficiency from 0.5 g of kaolinite. This same observation was also made in a study on the adsorption of organic micropollutants on bentonite[31] and in a study on the elimination of cadmium by adsorption on sodium and calcium bentonites[1].

These results could be explained by the increase in the mass of kaolinite which would increase the number of sites able to fix the dichromate ions; and the appearance of the bearing could be explained by the phenomenon of flocculation.

Influence of pH on adsorption: This study shows that at pH = 1.99 the adsorption of the dichromate is favorable, and at pH = 5.03 the adsorption of the dichromate is practically zero. These results could be explained by the fact that below the pH of the point of zero charge (pH = 4.7), this clay behaves as an anion fixer, thus dichromate. On the other hand, above the point of zero charge, it behaves as a cation fixer, which justifies the fact that the dichromate is not adsorbed[65].

Conclusion

This work had as a general objective the evaluation of adsorption capacity of dichromate ions by clay collected in the Impfondo locality. The mineralogy of this soil was determined by X-Ray diffraction, Infrared spectroscopy and differential thermal analysis and thermogravimetry analysis. The geotechnical (Atterberg limits and grain-size distribution) and the chemical properties (chemical composition, CEC, Tamm Fe and Mehra-Jackson Fe) were also studied. The surface properties (specific surface area and zero charge point) were evaluated. The adsorption isotherms and adsorption kinetics were carried out.

Impf clay consists mainly of kaolinite, but also illite, quartz, goethite, anatase, rutile and hematite. The particle size distribution corresponds to clay texture and offers the adsorption possibility. The surface properties (CEC, adsorption isotherm, adsorption kinetics, point of zero charge) have permitted to evaluate the adsorption capacity of Impf clay. This study showed that the adsorption isotherm of dichromate can be interpreted by the Langmuir and Freundlich models. Both models are to the extent of acceptability. The Freundlich model was used to calculate the Freundlich constant and the heterogeneity factor.

This study made it possible to conclude that the adsorption yield of dichromate on Impfondo kaolinite is low; it increases with the mass of the introduced kaolinite. And at a mass of 0.5 g of kaolinite in 25 ml of dichromate solution, the adsorption sites become saturated and the equilibrium is reached.

Following adsorption kinetics, the adsorption of dichromate is described by the second-order model. It was possible to determine the rate constant and the adsorption capacity of equilibrium dichromate ions.

The adsorption of dichromate is favored when the pH of the environment is much lower than that of the zero charge point of the kaolinite.

References

1. Ferhat Mourad (2012). Co-adsorption des métaux lourds sur la bentonite modifiée en présence de floculants minéral et biologique. Mémoire de magister, Université Mouloud Mammeri Tizi Ouzou, Algérie.
2. Achour S. and Youcef L. (2003). Elimination du cadmium par adsorption sur bentonites sodique et calcique. Larhyss Journal, ISSN 1112-3680, n°02, 68-81.
3. Sorgho B., Pare S., Guel B., Zerbo L., Traore K. and Persson I. (2011). Etude d'une argile locale du Burkina Faso à des fins de décontamination en Cu^{2+}, Pb^{2+}, Cr^{3+}. *Journal de la société ouest-africaine de chimie*, 16è année, n°031, 49-59.

4. Alvarez-Ayuso E., Garcia-Sanchez A. and Querol X. (2007). Adsorption of Cr (VI) from synthetic solutions and electroplating wastewaters on amorphous aluminium oxide. *Journal of Hazardous Materials*, 142(1-2), 191-198.

5. Ayari F., Srasra E. and Trabelsi-Ayadi M. (2004). Application des modèles de Langmuir et Freundlich aux isothermes d'adsorption des métaux lourds par l'argile purifiée. *J. Phys. IV France*, 122, 229-234.

6. Zachara J.M., Cowan C.E., Schmidt R.L. and Ainsworth C. C. (1988). Chromate adsorption by kaolinite. *Clays Clay Miner*, 36(4), 317-326.

7. Koppelman M.H. and Dillard J.G. (1980). Adsorption of Cr (NH3) 63+ and Cr (en) 33+ on clay minerals and the characterization of chromium by X-Ray photoelectron spectroscopy. *Clays and Clay Minerals*, 28(3), 211-216.

8. Errais E. (2011). Surface reactivity of natural clays: Study of the adsorption of anionic dyes (Doctoral dissertation, Strasbourg).

9. Toualakani B. (2016). Evaluation et risque pour la santé dû aux métaux Fe, Cr et PB dans les eaux souterraines du quartier Mayanga (Arrondissement N° 8 Madibou) Mémoire de Master. Ecole Normale Supérieure Université Marien Ngouabi (Congo Brazzaville).

10. Nimy Matsouele B.N. (2016). Présence potentielle dans l'eau du robinet des métaux As, Cd, Cr et Pb : Evaluation des risques toxicologiques pour la santé humaine. Cas du quartier DIATA, Mémoire de Master, Ecole Normale Supérieure, Université Marien Ngouabi (Congo Brazzaville).

11. Zecher D.C. (1969). Problems in replacing chromate as a corrosion inhibitor for open recirculating cooling waters. In Industrial process design for water pollution control, 89-92 New-York American Institute of Chemical Engineers.

12. Peter A.K. (1974). Sources and classification of water pollutants In Industrial pollution ed. by N. I. Sax. 197-217. New York, Van Nostrand Reinhold.

13. AFEE (1979). Les micropolluants minéraux dans les eaux superficielles continentales, rapport no.6: chrome-cuivre-nickel. Paris, Association Française pour étude des eaux.

14. Meisch H.U. and Schmitt-Beckmann I. (1979). Influence of tri-and hexavalent chromium on two Chlorella strains. Zeitschrift für Pflanzenphysiologie, 94(3), 231-239.

15. ATSDR (1993). Toxicological profile for chromium. Agency for Toxic Substances and Disease Registry, U.S. Department of Health and Human Services. Atlanta, GA. (revised 2012)

16. Cohen M.D., Kargacin B., Klein C.B. and Costa M. (1993). Mechanisms of chromium carcinogenicity and toxicity. *Critical reviews in toxicology*, 23(3), 255-281.

17. IARC (1990). Chromium and chromium compounds, International Agency for Research on Cancer (IARC). *Monogr. Eval. Carcinog. Risks Hum.*, 49, 49-214.

18. Davidson T., Kluz T., Burns F., Rossman T., Zhang Q., Uddin A. and Costa M. (2004). Exposure to chromium (VI) in the drinking water increases susceptibility to UV-induced skin tumors in hairless mice. *Toxicology and applied pharmacology*, 196(3), 431-437.

19. OEHHA (2009). Evidence on the developmental and reproductive toxicity of chromium (hexavalent compounds) Reproductive and Cancer Hazard Assessment Branch, Office of Environmental Health Hazard Assessment, California Environmental Protection Agency. http://www.oehha.ca.gov/prop65/hazard_ident/pdf_zip/chrome0908.pdf

20. OEHHA (2010). Proposition 65 Oral Maximum Allowable Dose Level (MADL) for Developmental and Reproductive Toxicity for Chromium (Hexavalent Compounds) Reproductive and Cancer Hazard Assessment Branch, Office of Environmental Health Hazard Assessment, California Environmental Protection Agency. http://www.oehha.ca.gov/prop65/law/pdf_zip/081210DraftMADLChromVI.pdf

21. ATSDR (2000). Toxicological profile for chromium, Agency for Toxic Substances and Disease Registry, U.S.. Department of Health and Human Services, Atlanta, GA.

22. Marks Jr J.G., Belsito D.V., DeLeo V.A., Fowler Jr J.F., Fransway A.F., Maibach H.I. and Storrs F.J. (2000). North American Contact Dermatitis Group patch-test results, 1996-1998. *Archives of Dermatology*, 136(2), 272-274.

23. United Nations (2017). Programme d'action national de lutte contre la désertification. www.unccd.int/ActionProgrammes/congo-fre2006.pdf lu le 17/09/2017

24. [NF P94-051] NF P 94-051(1993). Détermination des limites d'Atterberg. AFNOR.

25. NF P94 056 (1992). Analyse granulométrique des sols : méthode par tamisage. NF P94-057 (1992) Analyse granulométrique des sols : méthode par sédimentation, AFNOR

26. Carignan J., Hild P., Mevelle G., Morel J. and Yeghicheyan D. (2001). Routine analyses of Trace elements in geological samples using flow injection and low pressure on-line liquid chromatography coupled to ICP-MS: A study of geochemical reference materials, BR, DR-N, UB-N, AN-G and GH. *Geostandards Newsletter*, 25(2-3), 187-198.

27. Mehra O.P. and Jackson M.L. (1960). Iron oxide removal from soils and clays by a dithionite-citrate system buffered with sodium bicarbonate. *Clays Clay Miner.*, 7, 317-327.

28. Duchaufour P. and Souchier B. (1966). Note sur une méthode d'extraction combinée de l'aluminium et du fer libre dans les sols. *Science du Sol Bull. A.F.E.S*, 3, 161-175.

29. Hang P.T. and Brindley G.W. (1970). Methylene blue absorption by clay minerals. Determination of surface areas and cation exchange capacities (clay-organic studies XVIII). *Clays and clay minerals*, 18(4), 203-212.

30. NF X 31-130 (1999). Soil quality – Chemical methods – Determination of cationic exchange capacity (CEC) and extractible cations AFNOR.

31. Bougdah N. (2007). Etude de l'adsorption de micropolluants organiques sur la bentonite. Mémoire Magister, Université de Skikda, 17-18.

32. Assifaoui A. (2002). Etude de la stabilité des barbotines à base d'argile locale. Application aux formulations céramiques industrielles. Thèse de doctorat, Université ASSAN II AIN-CHOCK CASABLANCA, Maroc

33. Casagrande A. (1948). Classification and identification of soils. *Transactions of the American Society of Civil Engineers*, 113(1), 901-930.

34. Sanchez A.G., Ayuso E.A. and Blas O. (1999). Sorption of heavy metals from industrial waste water by low-cost mineral silicates. *Clay minerals*, 34(3), 469.

35. Brindley G.W. and Brown G. (1980). Crystal structures of clay minerals and their identification. *Mineralogical Society*, 497.

36. Caillère S., Hénin S. and Rautureau M. (1982). Minéralogie des argiles. Masson Ed., 1, 184.

37. Aparicio P. and Galan E. (1999). Mineralogical interference on kaolinite crystallinity index measurements. *Clays and Clay minerals*, 47(1), 12-27.

38. Sita P.M. (2013). Caractérisation minéralogiques de queldues sols argileux congolais Mémoire pour l'obtention du Certificat d'aptitude au Professorat de l'Enseignement Secondaire, Ecole Normale Supérieure Université Marien Ngouabi (Congo Brazzaville).

39. Moutou J.M., Mbedi R., Elimbi A., Njopwouo D., Yvon J., Barres O. and Ntekela H.R. (2012). Mineralogy and Thermal Behaviour of the Kaolinitic Clay of Loutété (Congo-Brazzaville). *Research Journal of Environmental and Earth Sciences*, 4(3), 316-324.

40. Jeanroy E. (1983). Diagnostic des formes du fer dans les pédogénèses tempérées. Thèse de Docteur d'Université, Université Nancy, I, 157.

41. Bouaziz R. and Rollet R.P. (1972). L'analyse Thermique: L'examen Des Processus Chimiques. Paris, Gauthiers-Villars, 2, 227.

42. Jouenne C.A. (2001). Traité de céramiques et matériaux minéraux. Edition Septima, Paris, 657.

43. Derie R., Ghodsi M. and Calvo-Roche C. (1976). DTA Study of the dehydration of synthetic goethite γ-FeOOH. *Journal of Thermal Analysis*, 9, 435-440.

44. Yvon J., Baudracco J., Cases J.M. and Weiss J. (1990). Elements of quantitative mineralogy in micro-analysis of clays. *Clay Materials, Structures, Properties and Applications*, 473-489.

45. Njopwouo D. (1984). Minéralogie et physico-chimie des argiles de Bomkoul et de Balengou (Cameroun). Utilisation dans la polymérisation du styrène et dans le renforcement du caoutchouc naturel. Thèse de Doctorat d'Etat, Université de Yaoundé, Cameroun, pp: 300.

46. Chamayou H. and Legros J.P. (1989). Les bases chimiques et minéralogiques de la science du sol. Agence de coopération culturelle et technique, Presses Universitaires de France, 584

47. Farmer V.T. and Russell J.D. (1964). The infra-red spectra of layer silicates. *Spectrochimica Acta*, 20(7), 1149-1173.

48. Rouxhet P.G., Samudacheata N., Jacobs H. and Anton O. (1977). Attribution of the OH stretching bands of kaolinite. *Clay Miner.,* 12, 171-178.

49. Van der Marel H.W. and Krohmer P. (1969). OH stretching vibrations in kaolinite, and related minerals. *Contributions to Mineralogy and Petrology*, 22(1), 73-82.

50. Elsass F. and Olivier D. (1978). Infrared and electron spin resonance studies of clays representative of the sedimentary evolution of the basin of Autun. *Clay Minerals,* 13, 299.

51. Saikia N.J., Bharali D.J., Sengupta P., Bordoloi D., Goswamee R.L., Saikia P.C. and Borthakur P.C. (2003). Characterization, beneficiation and utilization of a kaolinite clay from Assam, India. *Applied Clay Science*, 24, 93-103.

52. Prost R., Dameme A., Huard E., Driard J. and Leydecker J. P. (1989). Infrared study of structural OH in kaolinite, dickite, nacrite, and poorly crystalline kaolinite at 5 to 600 K. *Clays and Clay Minerals*, 37(5), 464-468.

53. Brindley G.W., Chih-Chun Kao, Harrison J.L., Lipsiscas M. and Raythatha R. (1986). Relation between structural disorder and other characteristics of kaolinites and dickites. *Clays and Clay Minerals,* 34, 239-249.

54. Vaculikova L., Plevova E., Vallova S. and Koutnik I. (2011). Characterization and differentiation of kaolinites from selected Czech deposits using infrared spectroscopy and differential thermal analysis Acta Geodyn. *Geomater*, 8, 59-67.

55. Lappi S.E., Smith B. and Franzen S. (2004). Infrared spectra of H216O, H218O and D2O in the liquid phase by single-pass attenuated total internal reflection spectroscopy. *Spectrochimica Acta Part A: Molecular and Biomolecular Spectroscopy*, 60(11), 2611-2619.

56. Van Olphen H. and Frippiat J.J. (1979). Data Handbook for Clay Minerals and Other Non Metallic Minerals. Pergamon Press, London.

57. Bertaux J., Frohlich F. and Ildefonse P. (1998). Multicomponent analysis of FTIR spectra: quantification of amorphous and crystallized mineral phases in synthetic and natural sediments. *Journal of Sedimentary Research*, 68(3), 440-447.

58. Wilson M.J. (1996). Clay Mineralogy: Spectroscopy and Chemical Determinative methods Ed. *Chapman and Hall*, London, 367.

59. Frost R.L and Johansson U. (1998). Combination bands in the Infrared spectroscopy of kaolins-A DRIFT spectroscopy study. *Clays and lay minerals*, 46(4), 466-477.

60. Hendershot W.H. and Lavkulich L.M. (1983). Effect of Sesquioxide Coatings on Surface Charge of Standard Mineral and Soil Samples 1. *Soil Science Society of America Journal*, 47(6), 1252-1260.

61. Rahajaharitompo R.L. (2004). Etude de la fertilité et de la fertilisation phosphatées des sols ferralitiques de Madagascar. Thèse de doctorat d'état es sciences naturelles, Université d'Antananarivo, Madagascar.

62. Giles C.H., Smith D. and Huitson A. (1974). A general treatment and classification of the solute adsorption isotherm. *Journal of Colloid and Interface Science*, 47(3), 755-765.

63. Yahiaoui N. (2012). Etude de l'adsorption des composés phénoliques des margines d'olive sur carbonate de calcium, hydroxyapatite et charbon actif. *Mémoire de magister, Université mouloud Mammeri Tizi Ouzou*, Algérie.

64. Assifaoui A. (2002). Etude de la stabilité des barbotines à base d'argiles locales. Application aux formulations céramiques industrielles, Thèse d doctorat, Faculté des sciences Casablanca Université Hassan II AIN CHOCK

65. Flogeac K. (2004). Etude de la capacité de rétention de produits phytosanitaires par deux solides modèles des sols. Influence de la présence de cation métallique. Thèse de doctorat, Université de Reims Champagne-Ardenne, France.